Multifractal properties of absorption probabilities

1988 J. Phys. A: Math. Gen. 21 2131

(http://iopscience.iop.org/0305-4470/21/9/026)

J. Phys. A: Math. Gen. **21** (1988) 2131-2142. Printed in the UK

Multifractal properties of absorption probabilities

M K Wilkinson† and R Brak‡

† Department of Physics, King's College, Strand, London WC2R 2LS, UK
‡ Department of Theoretical Physics, University of Oxford, 1 Keble Road, Oxford OX1 3NP, UK

Received 27 October 1987

Abstract. We calculate the surface absorption probabilities for particles diffusing onto perfectly absorbing substrates. The '$f(\alpha)$' formalism purporting to represent the multifractal properties of the absorption probabilities is discussed in the context of some simple test cases. The $f(\alpha)$ universality classes of several similar surfaces are studied and it is found that the $f(\alpha)$ curves for surfaces with the *same* fractal dimension are different.

1. Introduction

There is current interest in developing the understanding of a large class of physical phenomena possessing a property of self-similarity in some part of their structure. These phenomena include percolation clusters (Stauffer 1979, Kapitulnik *et al* 1983), random resistor networks (de Arcangelis *et al* 1986, Blumenfeld *et al* 1986), diffusion-limited aggregation (DLA) clusters (Meakin *et al* 1985, Turkevich and Scher 1985, Amitrano *et al* 1986, Meakin 1986a, Halsey *et al* 1986a) and phase-space trajectories of certain dynamical systems (Benzi *et al* 1984, 1985, Jensen *et al* 1985, Halsey *et al* 1986b). These phenomena are usually defined by some microscopic description, e.g. bond occupation for percolation or local differential equations of motion for dynamical systems. Following the microscopic description these phenomena are then understood in terms of a small number of macroscopic coordinates such as the first few moments of the distribution, e.g. the mean size of percolation clusters or average growth rate of the aggregate in DLA. Numerous studies (see, e.g., Stanley and Ostrowsky 1986) have shown that the above phenomena possess a very rich structure which is not fully captured by a macroscopic description.

To this end a mesoscopic description is required. A larger number of coordinates is necessary but not so many that the problem becomes unmanageable. This presents a fundamental problem: what are the necessary coordinates? Because of the self-similarity appearing in all these problems a simple fractal description has been used. However, a single fractal dimension is inadequate as exemplified by the comparison of percolation clusters (Sur *et al* (1977) use $d_f = d - \beta/\nu$) and DLA clusters (Meakin 1986b) in 3D which are very different structures and yet have the same fractal dimension. A generalisation of a simple fractal to the concept of a multifractal has been introduced in an attempt to provide the desired mesoscopic description.

We wish to make clear the distinction between the conceptual idea of a multifractal and any mathematical description which attempts to encode the idea. The conceptual idea is very simple (but suitably vague): a multifractal is an object which in some way

has many fractal dimensions associated with it. A fractal dimension is a rigorously defined quantity (i.e. the Hausdorff dimension; see Mandelbrot (1982), Falconer (1985) and Hutchinson (1981)). What is required is a clear definition of how many such dimensions can be associated with a single object. It is one of the objectives of this paper to study a particular attempt at the latter problem (Halsey *et al* 1986b) and determine how well it succeeds in satisfying the conceptual idea, especially for problems requiring numerical solutions.

Multifractal structure arises not necessarily from the object alone, but through the particular process taking place on the object. To be clear the object will be called the 'substrate set' and the process taking place on the object will be represented by a measure function, μ. For example, a random resistor network could be the substrate set whilst the value of the voltage across the resistors defines the measure function. It is important to note that the whole multifractal structure depends on the measure function chosen.

Halsey *et al* (1986b) proposed the following. The substrate set is partitioned into disjoint subsets, U_i, of diameter $|U_i| = l_i$. The diameter of a set U_i is defined as $\text{supp}\{|x-y|: x, y \in U_i\}$, where supp is the least upper bound and $|x-y|$ is the Euclidean distance between x and y. For each subset the following scaling ansatz for the measure function (which they take as a probability measure, $\mu(U_i) = p_i$) is made:

$$p_i \sim l_i^{\alpha} \tag{1.1}$$

and

$$N(\alpha) \sim l^{-f(\alpha)} \tag{1.2}$$

where $N(\alpha)\,\mathrm{d}\alpha$ is the number of subsets U_i, for which the exponent α lies in the interval $[\alpha, \alpha + \mathrm{d}\alpha]$. The multifractal description enters in the exponent $f(\alpha)$ which is now the fractal dimension of a subset of the substrate set for which the measure function has an exponent in the interval $[\alpha, \alpha + \mathrm{d}\alpha]$. We will refer to this as the $f(\alpha)$ representation. Halsey *et al* (1986b) further proposed a method of obtaining the set of exponents $\{\alpha, f(\alpha)\}$. We will call this the q formalism as it involves taking the qth moment of the probability measure.

In this paper we consider simple non-fractal substrate sets shown in figure 1 and simple fractal substrate sets whose generators are shown in figure 2. Using these

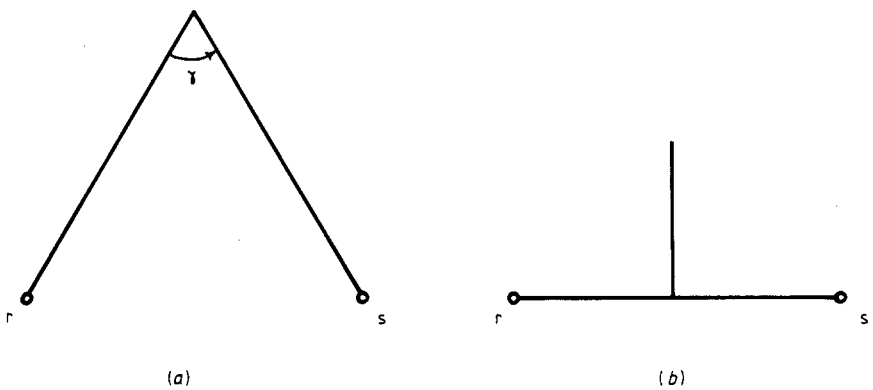

Figure 1. Non-fractal substrate sets: (a) a wedge with tip angle, $\gamma = \pi/3$, and (b) a spike ($\gamma = 0$). The points r and s are nearest neighbours because of the periodic boundary conditions.

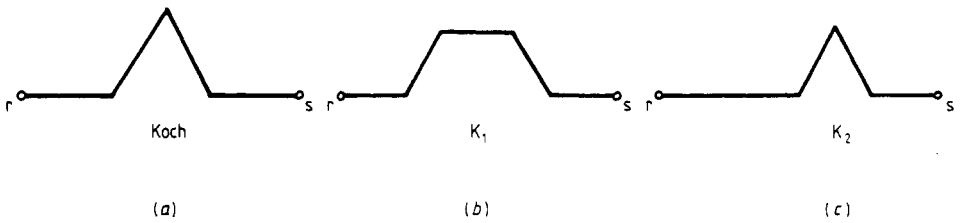

Figure 2. The generators of the fractal substrate sets: (*a*) the Koch curve, (*b*) the curve K_1 and (*c*) the curve K_2.

substrate sets we choose the measure function to be a probability measure. The probability measure, $\{p_i\}$, is determined by particles diffusing from infinity down onto the absorbing surface of the object, where p_i is the probability of a particle being absorbed on the surface site i. We will refer to it as the absorption measure. This work is a continuation of the work in Wilkinson and Brak (1987). Note that the substrate sets of the objects in figure 1 are not fractal on any length scale, whilst those in figure 2 are fractal in the limit of infinite recursion level. At any finite recursion level we loosely refer to them as incipient fractals or 'rough' surfaces. We pay particular attention to the meaning of the $f(\alpha)$ representation as determined by the q formalism and its success as a characterisation of multifractality. We are also interested in the transition from a rough to a fractal surface within the context of the $f(\alpha)$ representation.

The paper is arranged as follows. In § 2 we describe the methods used to compute the absorption measure and in §§ 3 and 4 we discuss the calculation of α and $f(\alpha)$ respectively. In § 5 we apply these methods to the incipient fractals of figure 2 and we conclude with § 6.

2. Numerical techniques

In this section we briefly discuss the relative merits of a number of different numerical methods for evaluating $\{p_i\}$ and we make explicit the nature of the boundary conditions and approximations inherent in our model. We begin by making the problem discrete by placing the substrate set and diffusing particles on a lattice. In the calculations below we use both the simple quadratic and triangular lattices depending on the nature of the surface. All of the features of the model are shown in figure 3, where there are

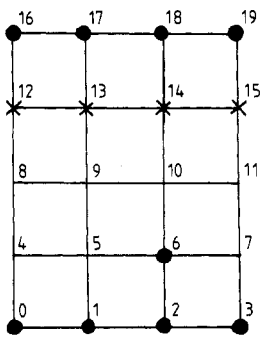

Figure 3. A simplified lattice showing the relevant features of the model. Full circles are absorbing sites and crosses are the release sites.

$N = 20$ sites in total. The substrate set consists of sites $S = \{0, 1, 2, 3, 6\}$ (note that site 2 can never be contacted because of the discretisation, i.e. $p_2 = 0$). The top boundary consists of sites $T = \{16, 17, 18, 19\}$ while sites $R = \{12, 13, 14, 15\}$ are the sites from which diffusing atoms are released. The lattice is imagined wrapped on a cylinder so that sites on the right-hand edge are nearest neighbours of those on the left-hand edge. (Below we discuss the effects of the positions of T and R. Ideally we would like the boundary effects to be negligible.)

We distinguish between interior sites (I) and boundary sites ($B = T \cup S$). We define π_{ij} as the probability of a diffusing particle stepping from i to j if it is already at i. Thus the π_{ij} are elements of the probability transition matrix **P** such that

$$\pi_{ij} = \begin{cases} q^{-1} & \text{if } i \neq j;\ i \in I \\ 0 & \text{if } i = j;\ i \in I \\ 0 & \text{if } i \neq j;\ i \in B \\ 1 & \text{if } i = j;\ i \in B \end{cases} \tag{2.1}$$

where q is the coordination number of the lattice. If a diffusing particle starts at an interior site it will eventually be absorbed by a boundary site. This problem is an example of an 'absorbing Markov chain'. In the standard theory of such problems (see, e.g., Kemeny and Snell 1960) one transforms the matrix **P** into canonical form

$$\mathbf{P} = \begin{pmatrix} \mathbf{1} & \mathbf{0} \\ \mathbf{D} & \mathbf{Q} \end{pmatrix} \tag{2.2}$$

which is simply obtained by relabelling the lattice sites so that the absorbing sites have the lowest labels. Matrix **D** describes how particles may step from the interior to the boundary. Matrix **Q** describes how particles diffuse within the interior. The fundamental matrix **F** is defined by

$$\mathbf{F} = \sum_{n=0}^{\infty} \mathbf{Q}^n = (\mathbf{1} - \mathbf{Q})^{-1} \tag{2.3}$$

and F_{ij} is the expected number of times that the diffusing particle will be at site j after starting from site i. Then the probability, A_{ij}, of starting at i and being absorbed at j is given by

$$\mathbf{A} = \mathbf{FD}. \tag{2.4}$$

The distribution $\{p_i\}$ follows trivially from (2.4) by averaging over the release sites.

From a practical point of view this method amounts to inverting an $N \times N$ matrix. Library routines are available to do this but the disadvantage is the large memory requirement. One can reduce this slightly by calculating $\mathbf{Q}^n$ directly by matrix multiplication, although this is rather slower.

A different approach stems from recognising the correspondence between our diffusion problem and the Dirichlet problem in electrostatics (see, e.g., Doyle and Snell 1983, Niemeyer *et al* 1984). We imagine that the sites B are points on a conductor held at zero potential and that the sites T are held at unit potential (we are assuming that sites R are adjacent to T). Since the electrostatic potential ϕ is a harmonic function for **P** the potential at site i is given by

$$\phi_i = \sum_{j \in \mathrm{NN}(i)} \pi_{ij} \phi_j \tag{2.5}$$

where NN(i) is the set of nearest neighbours of site i. Writing $(\phi_1, \phi_2, \ldots)$ as a column vector $\boldsymbol{V}$

$$\boldsymbol{V} = \mathbf{P}\boldsymbol{V} = \mathbf{P}^n \boldsymbol{V} \tag{2.6}$$

with n any integer. Now

$$\mathbf{P}^\infty = \begin{pmatrix} \mathbf{1} & \mathbf{0} \\ \mathbf{A} & \mathbf{0} \end{pmatrix} \tag{2.7}$$

since $\mathbf{Q}^\infty = \mathbf{0}$, so that the potential at the boundary determines the potential in the interior

$$\boldsymbol{V}_\mathrm{I} = \mathbf{A}\boldsymbol{V}_\mathrm{B} = \mathbf{F}\mathbf{D}\boldsymbol{V}_\mathrm{B} \tag{2.8}$$

or rewriting

$$\mathbf{F}^{-1}\boldsymbol{V} = (\mathbf{1} - \mathbf{Q})\boldsymbol{V}_\mathrm{I} = \mathbf{D}\boldsymbol{V}_\mathrm{B}. \tag{2.9}$$

Now the correspondence between absorption probabilities and potentials is established by

$$p_i \propto \sum_{j \in \mathrm{NN}(i)} \phi_j = \sum_{j \in \mathrm{NN}(i)} \sum_{k \in T} A_{jk} = \sum_{k \in T} \sum_{l \in \mathrm{NN}(k)} A_{li}. \tag{2.10}$$

The technique is to solve the system of equations (2.9) for $\boldsymbol{V}_\mathrm{I}$ given $\boldsymbol{V}_\mathrm{B}$. To do this we have used the well known method of successive over-relaxation (SOR) (see, e.g., Hageman and Young 1981). The only difficulty here is in selecting the value of the over-relaxation parameter, but using the semi-empirical adaptive procedure described by Hageman and Young we achieved very good results; with calculations having $|S| = 1024$ taking only a few minutes of CPU time (Cray 1S) at an accuracy of $10^{-6}\%$.

Another method we have investigated is the continuous-time random walks used by Turkevich and Scher (1985). This has the advantage of not requiring the T boundary sites and thus eliminating any bias from this source. However, the difficulty with this method is in evaluating the lattice Green functions as time tends to infinity. The infinite limit cannot be obtained numerically which leads to a systematic error. This error is small if the number of surface sites is small (in practice less than about 40). This size of surface was too small to be of use in this study. The final method that we considered is the Monte Carlo method extensively used in the calculation of absorption probabilities in DLA and other problems. In comparison with the methods described above this method is slow and we have not used it in any serious way.

We have studied the effect of the top cut-off boundary by adjusting it in two ways: first by changing the distance between the release sites and the substrate surface, and second by changing the distance between the release line and the upper absorbing surface. We find that the surface absorption probabilities rapidly approach limiting values as the boundary tends to the ideal case (i.e. the release line at infinity and the top absorbing surface infinitely further away still). This analysis shows that there is a maximum error introduced by the cut-off boundary of about 3%. This systematic bias has negligible effect on any conclusions we have drawn from the data. We have therefore taken the most expedient cut-off boundary.

In summary, there are various ways of calculating $\{p_i\}$ and we have tried those discussed above. We stress that all methods give the same results (to within the error bars) and our results have therefore been extensively cross-checked. We found the SOR method fastest and also very accurate. The results quoted in subsequent sections are from this method.

3. Calculation of α

A useful way of understanding α is by considering a 'wedge' which has a 'tip' angle, γ (see figure 1(a)). The spike in figure 1(b) is the limiting wedge obtained when $\gamma = 0$. If γ were equal to π the surface would of course be flat. As the substrate sets considered here are less than two dimensional a subset of the substrate set of diameter l_i will simply be referred to as 'the segment l_i'. The absorption measure, for a *flat* surface, for any segment, l_i, would behave like l_i^1, i.e. $\alpha = 1$. By solving Laplace's equation in two dimensions using conformal transformations it can be shown (Turkevich and Scher 1985) that α at the tip of a wedge is given by $\alpha = \pi/(2\pi - \gamma)$. The wedge is useful as an example because any singularity in the absorption measure can be thought of as arising from a wedge occurring on the segment l_i. This gives rise to a picture of an object, for which the absorption measure has many values of α, as consisting of many wedges. Numerically α is obtained in the same way as a fractal dimension is computed. The segment l_i, centred on the tip of the wedge is split into smaller segments, δ, of decreasing size, all centred on the wedge tip. For a given segment δ the total probability, $p(\delta)$, of the diffusing particle being absorbed within δ is determined numerically. Then α is given by

$$\alpha_i = \lim_{\delta \to 0} \frac{\mathrm{d} \ln p_i(\delta)}{\mathrm{d} \ln \delta} \tag{3.1}$$

i.e. by the slope of the log-log plot as $\delta \to 0$. We also propose to use

$$\alpha_i \approx \frac{\ln p_i(\delta)}{\ln \delta}. \tag{3.2}$$

Note that equation (3.2) is an equality in the limit as $\delta \to 0$, by (1.1). However, for finite δ, (3.2) is only approximate but, as will be shown below, it is in reasonable agreement with (3.1). It appears that the majority of studies use (3.2) either implicitly or explicitly. To test the effect of the lattice structure on α we calculated the absorption measure for a spike and wedge. The probability of the particle being absorbed in a segment δ, for a range of lengths, are shown in figure 4. From the slope (as $\delta \to 0$) the values of α were obtained and are given in table 1. The table includes the tip angle

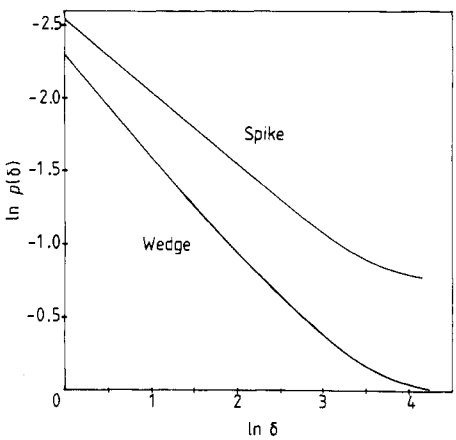

Figure 4. A plot of $\ln p(\delta)$ against $\ln \delta$ for the wedge and spike.

Table 1. Table of α estimates.

Angle	Exact α	$d \ln p / d \ln l$	$\ln p / \ln l$
$\gamma = 0$	1/2	0.5	0.46
$\gamma = \pi/3$	3/5	0.69	0.53
$\gamma = 3\pi/2$	2	2.2	1.8
$\gamma = 5\pi/6$	3	2.5	3.0

as well as the 'valley' angle (created by the periodic boundary conditions in the case of the wedge). The second column gives the exact values of α, the third column contains the values obtained from the small-δ slope, i.e. equation (3.1), and the final column gives the results obtained by using (3.2), where the probability, $p_i(\delta)$, is taken as the probability of the particle being absorbed on the lattice point on the tip of the wedge or spike. The results obtained by using (3.1) are in good agreement with the exact results, especially for the tip angles. The differences probably arise from the interference between the tip and valley and the systematic bias introduced by the boundary conditions (see § 2).

For the Koch curve (see § 5) we use only (3.2) to calculate α, where p_i is taken to be the probability of the particle being absorbed on the ith site. This approximation is justified by the reasonable agreement of the fourth column of table 1 with the exact results. The assumption is equivalent to replacing each lattice point of the Koch curve with a wedge. This assumption could be circumvented by increasing the number of substrate set points *keeping the geometry fixed* and using (3.1) to calculate each α. This procedure, however, is ineffective at high recursion level because of limitations of computing power. At low recursion level there is not a sufficient number of different α to make such effort worthwhile. For these reasons we use (3.2) throughout. Note that in the Koch curve the angles γ are all either $\pi/3$ or $\pi/6$ but their environments differ, resulting in screening, which may alter the nature of the α exponents.

In the q formalism, with $l_i = l$ for all i, $\alpha(q)$ is given by

$$\alpha(q) = \frac{\Sigma_i p_i^q \ln p_i}{\Sigma_i p_i^q \ln l}. \tag{3.3}$$

The qth moment is taken to ensure that the sums are dominated by one value of the probability, p^* and thus one value of α. This value of the probability is given by

$$p^*(q) = \left(\prod_i p_i^{p_i^q} \right)^{1/\Sigma p_i^q} \tag{3.4}$$

and for $q = 0$ this reduces to the geometric mean

$$p^*(0) = \left(\prod_i p_i \right)^{1/N} \tag{3.5}$$

where N is the number of sites. Note, that it is *only* in the limit $l \to 0$ that q does pick out only one probability. For finite l, the q formalism gives a sort of 'effective' α. Also, note that since $\alpha_{\min} = \ln p_{\max} / \ln l$ and $\alpha_{\max} = \ln p_{\min} / \ln l$ in these extremes the q formalism agrees with (3.2).

4. Calculation of $f(\alpha)$

Subsets of the substrate set with α in the interval $[\alpha, \alpha+d\alpha]$ are distributed, in the limit $l \to 0$, over sets of dimension $f(\alpha)$, where $f(\alpha)$ is a Hausdorff dimension. Our working definition is

$$f(\alpha) \approx -\ln N(\alpha)/\ln l \tag{4.1}$$

which has the same status as equation (3.2). The results obtained from equation (4.1) are plotted in figure 5 for the spike as a histogram. The smooth curve represents values of $f(\alpha)$ obtained from the q formalism:

$$f(\alpha(q)) = q\alpha(q) - \ln \Sigma p_i^q / \ln l. \tag{4.2}$$

The q formalism treats $f(\alpha)$ in the same way as it treats α for finite systems and is thus some kind of effective dimension for an effective α!

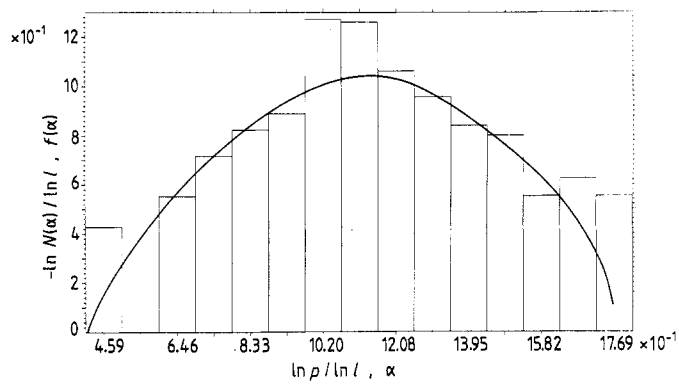

Figure 5. A plot of the histogram of $-\ln N(\alpha)/\ln l$ against $\ln p/\ln l$ for the spike. The smooth curve is the corresponding $f(\alpha)$ curve.

For the spike (with our boundary conditions), in the limit $l \to 0$, one expects rigorously (see Halsey *et al* 1986b, § C1) only three $f(\alpha)$ points, namely $\alpha = 1, f(\alpha) = 1$ corresponding to the flat region between the tip and the valley and two different α for the spike tip and valley both with $f(\alpha) = 0$. As shown clearly in figure 5, neither (4.1) nor the q formalism can reproduce this result. Both of these methods fail for finite l by making interpolations between the three points.

We do notice, however, that the histogram and the $f(\alpha)$ curve are very similar and for discrete finite-size systems they appear to give the same results. One advantage of the q formalism is that it gives a smooth interpolated curve for a finite set $\{p_i\}$. Finally, notice that the maximum of the q formalism $f(\alpha)$ curve has $f(\alpha)_{\max} > 1$ when in fact $f(\alpha)_{\max} = 1$. This is because of (1.2) which effectively replaces each point of the substrate set (on the lattice) by a reduced copy of itself and hence forces a fractal structure onto the rough substrate set (see Halsey *et al* 1986a, figure 2). However, as the number of lattice points defining the substrate set increases one would expect the computed $f(\alpha)_{\max}$ to tend to unity. This trend features in the case of the wedge where, for example, the numbers of substrate set points were 17, 53 and 161 and the corresponding fractal dimensions 1.289..., 1.204... and 1.156..., respectively.

5. Koch and other incipient fractals

In Wilkinson and Brak (1987) we have already seen that, for the Koch curve, the $f(\alpha)$ curve is relatively insensitive to the level of recursion and this is confirmed by the much more extensive calculation—up to recursion level 4—as shown in figure 6. Note that the curve passes through two known points: (i) the intercept $(\alpha_{\min}, 0)$ and (ii) the point $(\alpha_{\max}, -\ln 6/\ln l)$ which arises because there are always six points on the Koch curve having the minimum absorption probability. In addition the q formalism forces the maximum of the curve (by (1.2)) to have $f(\alpha)_{\max} = -\ln N/\ln l$ with N equal to the total number of points (i.e. $f(\alpha)_{\max} = d_f$, the fractal dimension of the substrate set). In figure 7 we compare the q formalism with the results obtained by using (4.1) where 1024 lattice points are used to define the surface. Here again the results are in reasonably good agreement.

The fact that (1.2) forces a recursive structure onto the substrate set is not a disadvantage for the Koch curve because of its inherent recursive structure. The consequent self-similarity is illustrated (see figure 8) by the penetration probability, this being the probability of a diffusing particle surviving a distance h (measured from the lowest point of the substrate set) before being absorbed. The cumulative surface

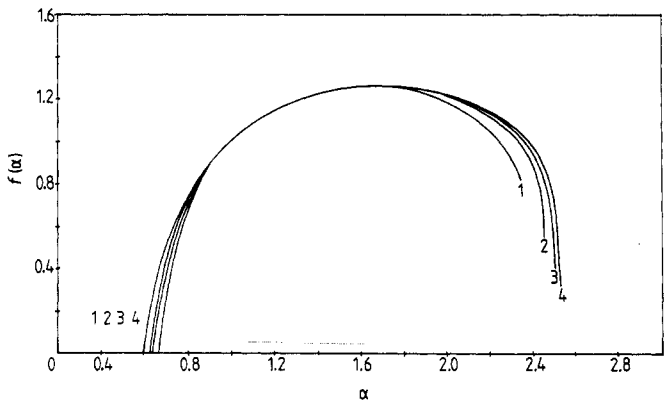

Figure 6. The $f(\alpha)$ curves for the Koch curve for the recursion levels 1, 2, 3 (512 points) and 4 (1024 points).

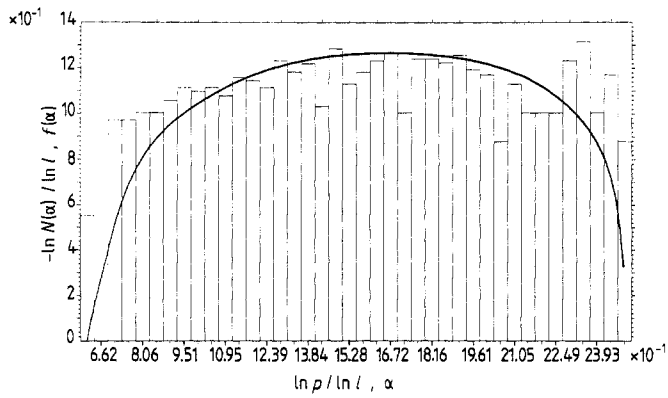

Figure 7. The histogram and $f(\alpha)$ curve for the Koch curve (recursion level 4).

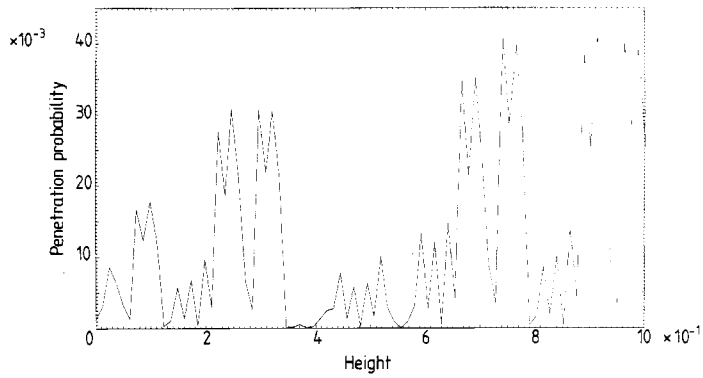

Figure 8. The penetration probability for the Koch curve. The height is measured from the lowest point of the curve upwards.

probability measured from the left-hand end of the curve (i.e. $p_{\text{cum}}(x) = \Sigma_{i=r}^{x} p_i$; see figure 2 for r), as shown in figure 9, also shows a self-similarity reminiscent of the 'devil's staircase' curve. The differential (along the substrate set) of the cumulative surface probability is p_i and it clearly shows the presence of more than one similarity ratio.

One of the principal motives of Halsey *et al* (1986b) was to give a universality class criterion. All of the different substrate sets studied so far give different $f(\alpha)$ curves. This is desirable as the substrate sets themselves are rather different. How similar do the curves have to be before they have the same $f(\alpha)$ curve and hence belong to the same universality class? In an attempt to answer this question we studied two additional curves, K_1 and K_2, whose generators are shown in figures 2(*b*) and 2(*c*). These are qualitatively the same as the Koch curve and furthermore these curves both have the *same* fractal dimension, $d_f = \ln 5/\ln 4 = 1.16\ldots$ (cf the Koch curve which has $d_f = \ln 4/\ln 3 = 1.26\ldots$). The $f(\alpha)$ curves for these geometries are contrasted with that of the Koch curve in figure 10. Notice that for small α (which corresponds to the tip region of the curves) the K_2 and Koch curve are quite similar. This is to be expected as both curves have the same tip angle, $\gamma = \pi/3$. This contrasts with the K_1

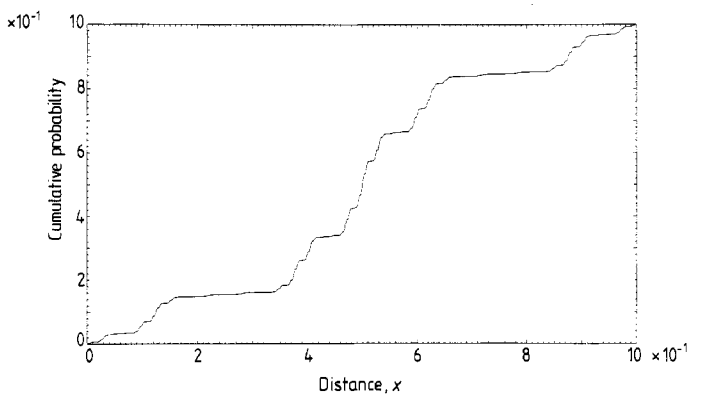

Figure 9. The cumulative surface probability, $\Sigma_{i=r}^{x} p_i$ for the Koch curve. The initial point $i = r$ is taken as point r of figure 2(*a*). Note the 'devil's staircase' structure of the graph.

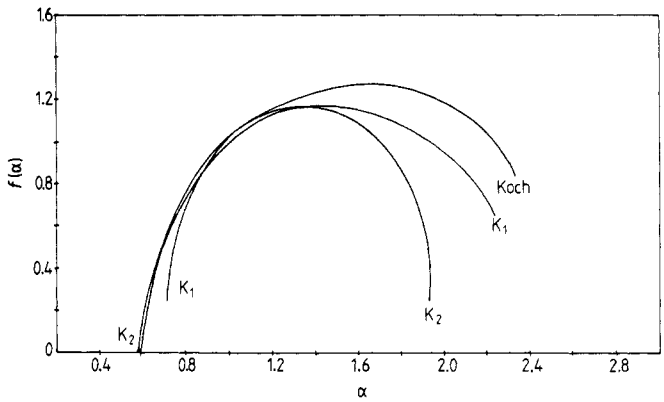

Figure 10. The $f(\alpha)$ curves for the Koch, K_1 and K_2 curves. Note, the K_1 and K_2 curves have the same fractal dimension but different $f(\alpha)$ curves.

curve which tends to have a larger α as $\gamma = 2\pi/3$ for the tip region. Where the three curves might differ the most, *with respect to their absorption measures*, is in the valley regions (i.e. large α) and this is just where the $f(\alpha)$ curves deviate the most.

6. Conclusions

In this paper we have calculated the absorption probabilities for particles diffusing onto perfectly absorbing boundaries using the SOR method. We have studied the $f(\alpha)$ representation of Halsey *et al* (1986b) by means of simple test substrates (figure 1). We have contrasted the results of the q formalism with simple working definitions of α and $f(\alpha)$ (see (3.2) and (4.1)). In an extension of the work of Wilkinson and Brak (1987) we have calculated $\{p_i\}$ for the Koch curve with up to 1024 points on the surface (recursion level 4). We have calculated other quantities (figures 8 and 9) associated with this curve and are able to see explicitly 'multifractal' scaling. To test for universality in the $f(\alpha)$ curves we have examined related fractal boundaries.

It appears that the principal problem with using the $f(\alpha)$ representation lies in the relation between the discrete nature of the substrate sets and the limiting behaviour as $\delta \to 0$ and $l \to 0$ (in that order). The limit $\delta \to 0$ (to obtain the α) presents little problem. For the wedge and the spike it is simple to implement numerically and the discrete lattice structure gives good results for the exponents α. For the Koch, K_1 and K_2 substrate sets this procedure could also be used but would only give a very small number of α. There is a strong possibility of losing the interpretation arising from (3.1) if (3.2) is used in its place. However, using (3.2) gives as many α as there are points on the substrate set and *if* each lattice point has a wedge structure at some lower recursion level then (3.2) is a good numerical approximation and, furthermore, the interpretation is not lost. We have assumed this to be the case for the incipient fractal curves.

The limit $l \to 0$ is far more difficult to implement without jeopardising the interpretation of $f(\alpha)$. Clearly it fails in the case of the wedge and the spike both when (4.1) and when the q formalism is used. This appears to be because (1.2) forces a fractal structure on the substrate set whether it is fractal or not. That this is so follows directly from (1.2) and can be clearly seen in the variation of $f(\alpha)_{\max}$ with recursion level for

the wedge (and spike): $f(\alpha)_{\max}$ is rigorously one but (1.2) forces it to be the fractal dimension of an object whose *generator* is the wedge (or spike). Because of this the $f(\alpha)$ representation cannot, for discrete finite-size systems, be used as a criterion for the existence of multifractal structure. It is also suspect even for fractal substrate sets that $f(\alpha)$ remains true to its interpretation. The q formalism gives similar results for the substrate sets to those obtained through the working definitions (3.2) and (4.1).

The penetration probability and the cumulative surface probability for the Koch curve both have a self-similar structure. However, the graphs do not have a single similarity ratio and this, combined with the self-similar structure, suggests they must be multifractal. We emphasise that a $f(\alpha)$ curve can be obtained *numerically* even when there is no hint of multifractality in the problem.

The $f(\alpha)$ representation does provide a mesoscopic description in so far as the $f(\alpha)$ curves for the K_1 and K_2 substrate sets are different despite the two substrate sets having the same fractal dimension.

Acknowledgments

MKW is grateful to the SERC for financial support. RB is grateful to the Oxford Theoretical Physics Department for hospitality.

References

Amitrano C, Coniglio A and di Liberto F 1986 *Phys. Rev. Lett.* **57** 1016
Benzi R, Paladin G, Parisi G and Vulpiani A 1984 *J. Phys. A: Math. Gen.* **17** 3521
—— 1985 *J. Phys. A: Math. Gen.* **18** 2157
Blumenfeld R, Meir Y, Harris A B and Aharony A 1986 *J. Phys. A: Math. Gen.* **19** L791
de Arcangelis L, Redner S and Coniglio A 1986 *Phys. Rev.* B **34** 4656
Doyle P G and Snell J L 1983 *Random Walks and Electrical Networks* (Washington, DC: Mathematical Association of America)
Falconer K J 1985 *The Geometry of Fractal Sets* (Cambridge: Cambridge University Press)
Hageman L A and Young D M 1981 *Applied Iterative Methods* (New York: Academic)
Halsey T C, Meakin P and Procaccia I 1986a *Phys. Rev. Lett.* **56** 854
Halsey T C, Jensen M H, Kadanoff L P, Procaccia I and Shraiman B I 1986b *Phys. Rev.* A **33** 1141
Hutchinson J E 1981 *Indiana Univ. Math. J* **30** 713
Jensen M H, Kadanoff L P, Liebchaber A, Procaccia I and Stevans J 1985 *Phys. Rev. Lett.* **55** 2798
Kapitulnik A, Aharony A, Deutscher G and Stauffer D 1983 *J. Phys. A: Math. Gen.* **16** L269
Kemeny J G and Snell J L 1960 *Finite Markov Chains* (New York: van Nostrand)
Mandelbrot B B 1982 *The Fractal Geometry of Nature* (San Francisco: Freeman)
Meakin P 1986a *Phys. Rev.* A **34** 710
—— 1986b *On Growth and Form: Fractal and Non-fractal Patterns in Physics* ed H E Stanley and N Ostrowsky (Dordrecht: Martinus Nijhoff) p 111
Meakin P, Stanley H E, Coniglio A and Witten T A 1985 *Phys. Rev.* A **32** 2364
Niemeyer L, Pietronero L and Wiesmann H J 1984 *Phys. Rev. Lett.* **52** 1033
Stanley H E and Ostrowsky N (ed) 1986 *On Growth and Form: Fractal and Non-fractal Patterns in Physics* (Dordrecht: Martinus Nijhoff)
Stauffer D 1979 *Phys. Rep.* **54** 1
Sur A, Lebowitz J L, Marro J, Kalos M H and Kirkpatrick S 1977 *J. Stat. Phys.* **15** 345
Turkevich L A and Scher H 1985 *Phys. Rev. Lett.* **55** 1026
Wilkinson M K and Brak R 1987 *J. Phys. A: Math. Gen.* **20** L307